

# External-cavity tunable mid-infrared laser using off-band surface-emitting Bragg grating coupler

H. L. Zhang,<sup>a)</sup> C. Peng, A. Seetharaman, G. P. Luo, and Han Q. Le<sup>b)</sup>

Photonic Device and System Laboratory, Department of Electrical and Computer Engineering, University of Houston, Houston, Texas 77204-4005

C. Gmachl,<sup>c)</sup> D. L. Sivco, and A. Y. Cho

Bell Laboratories, Lucent Technologies, Murray Hill, New Jersey 07974

(Received 9 September 2004; accepted 30 January 2005; published online 9 March 2005)

An external-cavity laser using an integrated two-segment design allows broad and continuous wavelength tuning with independent control of power and wavelength. The laser has a gain segment and a surface-emitting Bragg grating segment that was designed to be off-band for zero reflection inside the cavity, and with a strong free-space coupling to an external mirror to form a linear cavity. Wavelength control was achieved with a combination of coarse and broad wavelength tuning (140 nm) with the external mirror, and continuous, fine wavelength tuning via current-induced phase shift in the Bragg grating. Separate controls of the two segments allowed wavelength fine tuning without power variation and vice versa. The concept was applied to a 7  $\mu\text{m}$  laser, and is applicable to other wavelength. © 2005 American Institute of Physics. [DOI: 10.1063/1.1885188]

Among various designs for external cavity tunable semiconductor lasers, the approach with an integrated off-band surface emitting Bragg grating (SEBG) coupler as illustrated in Fig. 1(a) and described in several works<sup>1-5</sup> has the appeal of being compact, eliminating the need for an external grating. However, while broad wavelength tuning was demonstrated for this type of laser,<sup>1-5</sup> there was no description of its fine wavelength tuning and control. Mirror tilting will result in longitudinal mode hopping, unless the cavity length is also tuned. Relying purely on the mechanical control of both mirror angle and cavity length for accurate wavelength tuning can be challenging. In fact, many telecom lasers use injection current or temperature as more convenient mechanisms for fine wavelength control.

This paper describes a two-segment approach that differs from previous works<sup>1-5</sup> in which the SEBG serves not only as a wavelength-selective optical coupler, but also as a phase segment for fine wavelength control and tuning. Injecting a current into this segment, which is independent from the gain segment, causes an optical phase shift that results in a change of the lasing wavelength. This change can be controlled on a much finer scale than that with mirror tilting. The approach thus allows a hybrid of coarse, broad wavelength tuning with the external mirror, and continuous, fine wavelength tuning with the integrated SEBG. Multisegment monolithic lasers with separate current injection controls are common for telecom applications, but this concept has not been applied to this type of laser.

The experiments involved mid-IR (MIR) quantum cascade (QC) laser.<sup>6</sup> As crucial and stringent as in telecom, MIR spectroscopic applications require not only broad but also fine and accurate wavelength tuning. This has been the interest in previous external cavity MIR laser work,<sup>7</sup> and a similar

approach<sup>8</sup> also used a two-segment device but with a conventional external planar grating rather than a SEBG.

In principle, the basic idea is simply an SEBG that diffracts light into free space at an angle  $\theta$  off the normal axis as illustrated in Fig. 1(a), which is governed by the relation

$$\Lambda n_{\text{eff}} + \Lambda \sin(\theta) = \lambda, \quad (1)$$

where  $\lambda$  is the free-space wavelength,  $\Lambda$  is the grating period, and  $n_{\text{eff}}$  is the effective phase index. The Bragg grating is designed so that its intrawaveguide reflection spectrum (second order) is outside the device optical gain band (i.e., off-band or off-resonance) to avoid self-oscillation. An external feedback mirror completes the linear cavity. Tilting the mirror results in wavelength tuning in accordance with Eq. (1). If the mirror angle is fixed, a small change of  $n_{\text{eff}}$  results

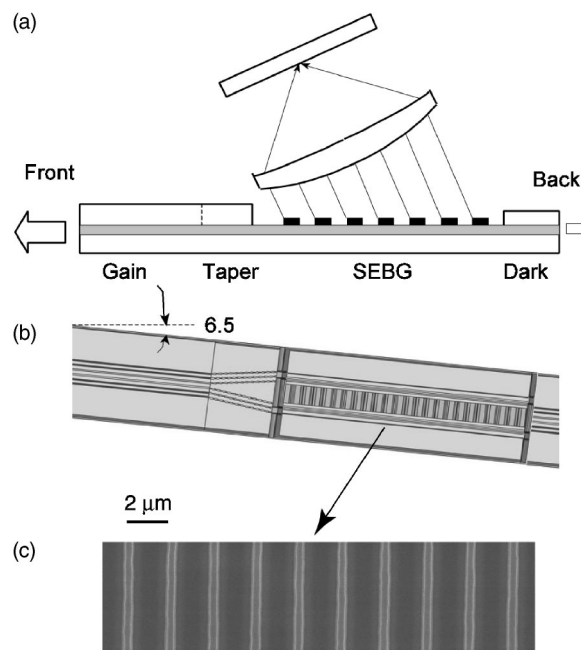


FIG. 1. (a) Schematic side view of the external cavity laser with off-band surface-emitting Bragg grating coupler; (b) Schematic top view of the device (the drawing is not to scale); (c) SEM image of the gratings.

<sup>a)</sup>Electronic mail: hlzhang@svec.uh.edu

<sup>b)</sup>Author to whom correspondence should be addressed. Electronic mail: hqle@uh.edu; also with Protea Corp., Sugar Land, Texas 77479, info@proteacorp.com

<sup>c)</sup>Current address: Department of Electrical Engineering and PRISM, Princeton University, Princeton, New Jersey 08540.

in a phase shift and wavelength change according to

$$\Delta\Delta n_{\text{eff}} = \Delta\lambda. \quad (2)$$

For off-band design,  $n_{\text{eff}}$  is approximately the phase refractive index of the SEBG, which can be current-tuned.

In practice, laser engineering requires consideration of the complete cavity, including the gain segment, the design of SEBG, the diffracted optical beam profile, coupling lens and mirror, and if needed, additional approaches to suppress self-oscillation. A detailed discussion is beyond the length of this paper; but key considerations led to three features that are crucial to this work and distinctive compared with the previous works.<sup>1-5</sup> These features are: (i) a separate control of the SEBG from the gain segment as mentioned above, (ii) the in-plane tilted facets for both segments and a dark segment as illustrated in Fig. 1(b), and (iii) SEBG window width that is substantially wider ( $\sim 35 \mu\text{m}$ ) than the gain segment ridge waveguide ( $15 \mu\text{m}$ ) that allows more efficient optical coupling and mirror feedback without involving higher order transverse modes.

The gain-SEBG integrated chips were fabricated from a 7- $\mu\text{m}$  Type I QC wafer, of which the structure is similar to those reported in Ref. 9. It consists of a 10-nm  $n+$  InGaAs contact layer, a 2.7- $\mu\text{m}$  InGaAs/AlInAs  $n$ -doped top cladding layer, and a 2.35- $\mu\text{m}$  InGaAs/InAlAs active core on an  $n+$  InP substrate, which is also the bottom cladding. A schematic top view of the device is shown in Fig. 1(b). It consists of a 15- $\mu\text{m}$  wide, 0.6-mm long ridge waveguide optical gain segment, followed by a 0.5-mm-long taper that joins the gain segment to the SEBG, which is 50- $\mu\text{m}$  wide and 2-mm long. A 0.2-mm long, 15- $\mu\text{m}$  wide dark region terminates the device. In the wafer plane, the entire device is tilted by  $6.5^\circ$  with respect to the normal of the facet. Both the dark region and the facet tilting are designed to suppress the Fabry-Perot self-oscillation.

The design and fabrication of the SEBG was crucial. The top cladding layer of the region was first etched down by 1  $\mu\text{m}$  in aged HBr:HNO<sub>3</sub>:H<sub>2</sub>O(1:1:10) to expose the evanescent wave. The gratings were subsequently patterned with two-beam holographic lithography using 362.8-nm Ar<sup>+</sup> laser. The gratings were transferred from photoresist to the semiconductor by wet etching with the same chemical solution to a depth of  $\sim 0.7 \mu\text{m}$ . Figure 1(c) shows a SEM image of the gratings. The grating period of 2.055  $\mu\text{m}$  was chosen so that its reflection is at 6.4  $\mu\text{m}$ , outside the laser 6.9–7.1- $\mu\text{m}$  gain band, and yet the surface-emitting angle  $\theta$  is sufficiently small to minimize astigmatism and optical aberration of the beam through the coupling lens. The grating tooth duty cycle and depth were designed to have large coupling strength for efficient external cavity coupling, which is  $\sim 12 \text{ cm}^{-1}$  in this case, but also with small reflectivity,  $< -23 \text{ dB}$  for in-band radiation to avoid second-order lasing.

The gain ridge waveguides were defined with wet etching to a depth of 10  $\mu\text{m}$ . A 400-nm-thick SiO<sub>2</sub> layer was deposited as an electrical insulation layer. A 42- $\mu\text{m}$  wide window was opened on the grating, and a 10- $\mu\text{m}$  window was opened on the gain segment for metal deposition. The two segments have different electrical contacts, separated by a stripe of the SiO<sub>2</sub> layer. No other processing was done, e.g., ion bombardment, to enhance electrical isolation. Lateral current injection was used in the grating coupler region. Here, the metal contacts cover only the edges of the grating

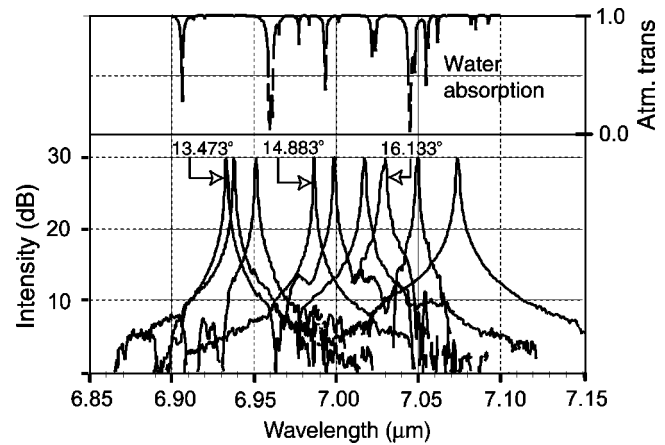


FIG. 2. Bottom: Laser wavelength tuning spectra obtained by tilting the mirror angle; a few angle values are shown. Top: Calculated atmospheric transmission for a distance comparable with the laser cavity roundtrip in air, showing strong water absorption. Wavelength tuning measurements were conducted within the water vapor windows.

for about 3.5  $\mu\text{m}$  on each side. A 35- $\mu\text{m}$  wide window was opened on the grating center using lift-off to allow surface emission.

The device was bonded on a submount, and mounted inside a LN<sub>2</sub> Dewar and operated  $\sim 80 \text{ K}$ . The coupling lens and mirror were external to the Dewar and at room temperature. The longitudinal mode spacing is  $\sim 2.5 \text{ GHz}$ . The gain and SEBG segments were driven with different electrical supplies. The laser was operated in pulsed mode with pulse width  $\sim 200 \text{ ns}$  and repetition rate of 250 kHz.

The quality of the surface-emitting beam is crucial. This beam was not directly measured in the external cavity configuration, but could be studied by overdriving the device to induce FP oscillation. Under this condition, the SEBG simply served as an output coupler without any wavelength selectivity. The off-normal beam was found to be diffraction-limited both along the length and width of the grating.

The coarse wavelength tuning spectra obtained by tilting the mirror angle are shown in Fig. 2 (bottom). Also shown at the top is the HITRAN® calculation of atmospheric water absorption. Since the laser cavity was in the ambient atmosphere and the water effects were pronounced, studies of the wavelength tuning behavior were conducted in the water windows. The tuning range of 140 nm was mostly limited by the wafer gain band as inferred from the amplified spontaneous emission, and partially by parasitic FP oscillation. The slope of wavelength vs mirror angle corresponds to a group velocity index of  $\sim 3.142$ . The linewidth was limited by the instrument resolution. However, it was sufficient to resolve more than two longitudinal modes. Results in this work were for mostly single mode operation.

The focus of this paper is the fine wavelength tuning behavior. By injecting current  $I_{\text{BG}}$  into the SEBG, the wavelength (or optical frequency) could be tuned as shown in Fig. 3. The frequency shift is sufficient to cover a few longitudinal modes. The inset shows several BG phase tuning spectra. Interestingly, the shift did not exhibit monotonic behavior. The frequency (open circles) increased modestly initially but decreased afterward. This behavior appears to be a sum of two effects with opposite signs: the carrier/voltage effect, and the thermo-optic effect. The latter is more dominant and can be obtained alone by simply introducing a time delay between the gain pulse current  $I_g$  and the SEBG current.<sup>8</sup> For

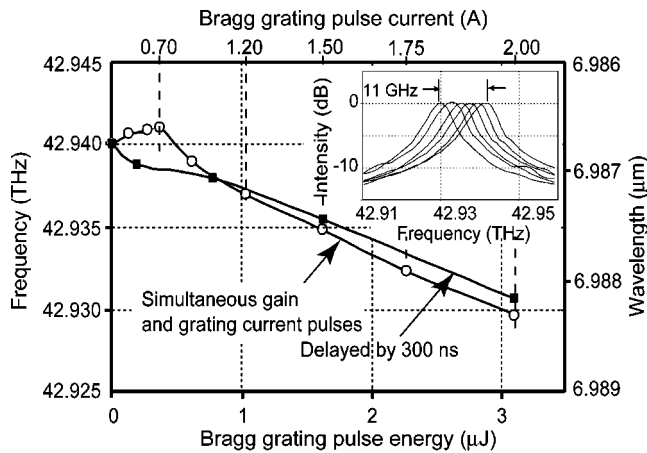


FIG. 3. Fine wavelength tuning behavior as a function of the surface-emitting Bragg grating injection current. The top axis shows the grating peak current, the bottom shows its pulse energy. Open circles: gain current  $I_g$  and grating current  $I_{BG}$  applied simultaneously. Filled square:  $I_g$  was delayed by 300 ns. Inset: examples of fine-tuning spectra.

300-ns delay, the pulses were not overlapped and the carrier/voltage effect vanished, while the residual heat was still substantial for the thermo-optic effect. The results are shown as the filled squares, exhibiting monotonic behavior as expected. Owing to the time delay, the effect is weaker than that without delay.

The magnitude of these effects is sufficient for applications. For the thermo-optic effect, the  $\Delta n_{\text{eff}}$  observed is  $\sim 7.5 \times 10^{-4}$ , which corresponds to an estimated temperature rise of  $\sim 5.5$  K. At low  $I_{BG}$  ( $< 0.75$  A), the carrier/voltage effect appears to dominate. Although its behavior and magnitude are comparable with the carrier plasma effect in interband diode lasers, the material used here is quantum cascade and the mechanism may be more complex. But since it is small and saturates for  $I_{BG} > 0.75$  A, it is not important here.

Without separate controls of gain and SEBG, this laser would suffer the typical problem of correlated and simultaneous wavelength and power variation, e.g., wavelength chirp associated with power modulation. Multisegment lasers are designed to overcome this problem. Ideally, current injection in the SEBG should not affect the power. However, in this case, since the SEBG is monolithically fabricated from the same wafer structure with active region, and the electrical isolation between the two segments is not perfect, current injection caused some unwanted power variation as shown in Fig. 4 (filled squares). This variation however, can be easily compensated with a gain current  $I_g$  correction to maintain a constant power as indicated (open squares). Vice versa, varying the gain current for power change causes wavelength shift as shown (filled circles), which can be compensated with an  $I_{BG}$  adjustment to maintain constant wavelength as indicated (open triangles).

Thus, this 2-segment structure allows combining  $I_g$  and  $I_{BG}$  to achieve independent and arbitrary control of power and wavelength. This is similar to most multi-segment lasers, which require a “look-up” table of combinations of various injection currents to control power and wavelength. A previous work [8] has shown that thermo-optic correction can be performed at 10’s kHz bandwidth, depending on the thermal characteristic of the device; here, the wavelength correction was measured from 100 to 400 Hz bandwidth.

In summary, this paper shows that 2-segment off-band surface emitting Bragg-grating coupled external cavity laser

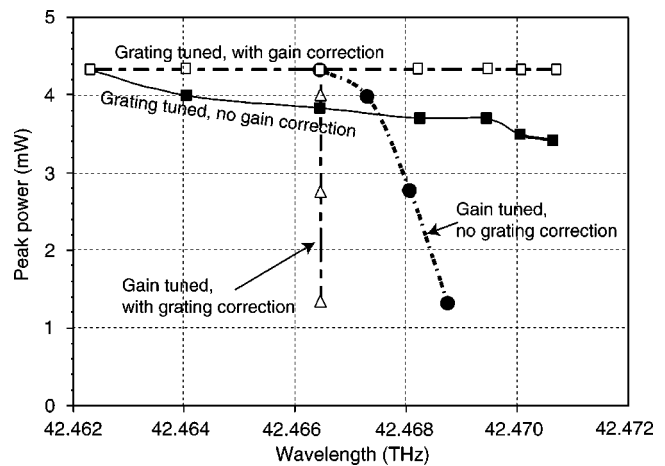


FIG. 4. External cavity laser power and wavelength control by combining gain and the Bragg grating (BG) segment currents. Filled squares: power variation as wavelength was tuned with BG segment alone. Open squares: Power corrected (maintained constant) with a gain current correction. Varying the power via the gain segment alone also resulted in unwanted wavelength shift (filled circles), which can be corrected with the BG current for constant wavelength (open triangles).

is a promising approach for broad, continuous, and fine wavelength tuning with independent power control. The essence is to have separate electrical controls for the SEBG segment and the gain segment. The former is used mainly for fine wavelength tuning; the latter is for power control. This is different from previous works,<sup>1-5</sup> which focused only on coarse and broad wavelength tuning with mirror. Theoretical considerations indicate that this laser can be even more compact if the device is operated at room temperature to allow shorter coupling distance to the mirror, e.g.,  $< 1$  cm, which can also be MEMS-controlled. An advantage would be larger longitudinal mode spacing for better side mode suppression. The MIR QC laser here was operated at low temperature, but high-power, high temperature devices are possible.<sup>10</sup> Also, the concept was experimentally demonstrated for MIR, but it is applicable to any other wavelength.

This work was supported by the U.S. Army Research Office/DARPA under Contract No. DAAD190010361, the U.S. Air Force Research Laboratory/DARPA under Contract No. F33615-02-C-1139, and the State of Texas THECB under an ATP program and the Texas Center for Superconductivity and Advanced Materials.

<sup>1</sup>J. Jiang, O. Smolski, C. Roychoudhuri, E. Portnoi, G. Venus, I. Gadjiev, and J. Mckillop, *Electron. Lett.* **35**, 1847 (1999).

<sup>2</sup>M. Uemukai, T. Suhara, K. Yutani, N. Shimada, Y. Fukumoto, H. Nishihara, and A. Larsson, *IEEE Photonics Technol. Lett.* **12**, 1607 (2000).

<sup>3</sup>Y. Hu, A. Gubenko, G. Venus, I. Gadjiev, N. Il'inskaja, S. Nesterov, E. Portnoi, M. Dubov, and I. Khrushchev, *Appl. Phys. Lett.* **82**, 4236 (2003).

<sup>4</sup>O. Smolski, J. Jiang, C. S. Roychoudhuri, E. Portnoi, G. Venus, and J. Bullington, *Proc. SPIE* **4651**, 59 (2002).

<sup>5</sup>K. Kim, S. Lee, O. Smolski, and P. J. Delfyett, *Opt. Lett.* **29**, 1273 (2004).

<sup>6</sup>See, for example, J. Faist, F. Capasso, C. Sirtori, D. L. Sivco, and A. Y. Cho, *Semiconductors and Semimetals* (Academic, New York, 2000), Vol. 66, pp. 1-83.

<sup>7</sup>C. Peng, G. P. Luo, H. Q. Le, *Appl. Opt.* **42**, 4877 (2003).

<sup>8</sup>C. Peng, H. L. Zhang, and H. Q. Le, *Appl. Phys. Lett.* **83**, 4098 (2003).

<sup>9</sup>C. Gmachl, N. Owschimikow, A. Belyanin, A. M. Sergent, D. L. Sivco, M. L. Peabody, A. Y. Cho, and F. Capasso, *Appl. Phys. Lett.* **84**, 2751 (2004).

<sup>10</sup>A. Evans, J. S. Yu, J. David, L. Doris, K. Mi, S. Slivken, and M. Razeghi, *Appl. Phys. Lett.* **84**, 314 (2004).